CHAPTER 7

Chapter 7

Niobium(V) Peroxo Complexes as Potent Inhibitors of Acid Phosphatase Activity

Contents

The developed monomeric as well as polymer supported triperoxoniobium complexes were screened for their effect on function of acid phosphatase (ACP). Detailed kinetic analysis revealed that monomeric pNb compounds are potent mixed type of inhibitors of ACP, whereas, the pNb macro complexes behave as classical non-competitive inhibitors of the enzyme.

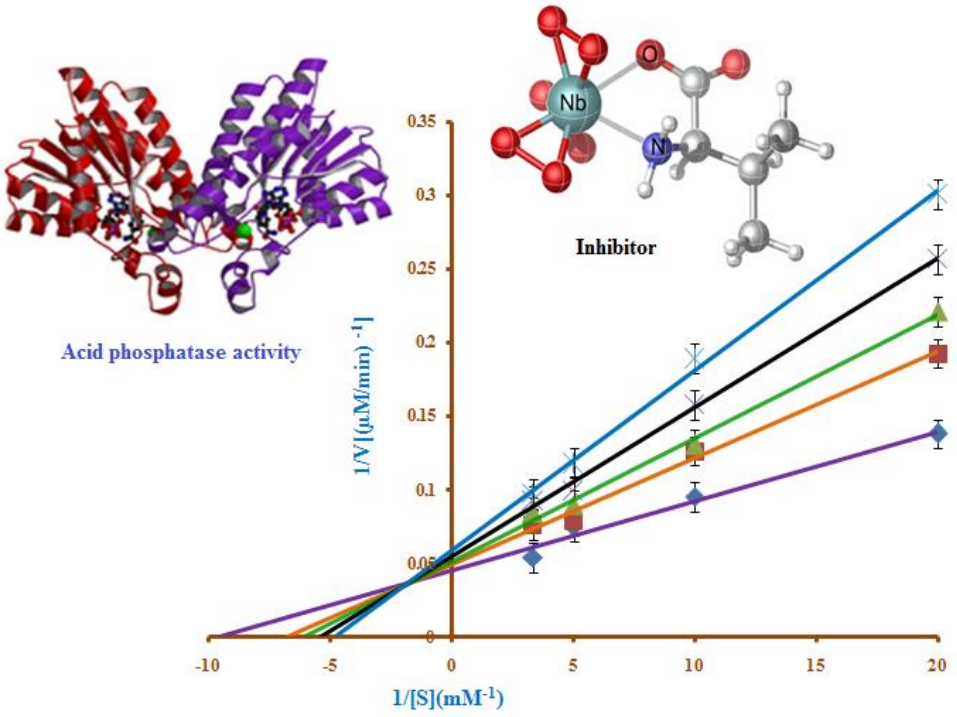

7.1 Introduction

Phosphorylation/dephosphorylation of a biomolecule is a key reaction in biology as phosphate ester bond functions as an extremely important linkage within the living cells [1-4]. It participates in storage and transfer of the genetic information, carries chemical energy and regulates the activity of enzymes and signalling molecules in the cell [1]. Enzymes capable of acting on ester bonds and catalyzing the cleavage of phosphate esters constitute the range of enzymes collectively named phosphatases. In fact, phosphohydrolases have become a key target for studying metabolism [5,6], for modifying cell signalling [6-8] and for treatment of diseases owing to the pivotal role of phosphatases in signal transduction pathways [5,6,9].

Specifically, vanadate and compounds of vanadium including pV are well-known inhibitors of phosphatases and their ability to inhibit phosphohydrolase enzymes has been recognized as crucial to understanding the bioactivity of vanadium, such as their anti-diabetic activity [10,11]. The inhibitory effects of vanadate have stimulated the development and testing of many other systems including pMo and pW derivatives as phosphatase inhibitors [12-20]. However, no reports appear to exist so far, on *in vivo* or *in vitro* effect of peroxoniobium species on phosphohydrolases although, according to a recent report, vanadate and niobate are strong inhibitors of the sarcoplasmic reticulum (SR) Ca^{2+}-ATPase that can affect calcium homeostasis, cell signalling and many other cellular processes [21].

The inhibition of phosphatases by vanadate and pV compounds has been the topic of several reviews [6,14,22-24]. The efficacy of vanadium based phosphatase inhibitors have been comprehensively reviewed by McLauchlan and co-workers recently [6], in which it has been observed that, notwithstanding the existence of numerous studies dealing with relative inhibitory potency such as EC_{50} of V as well as Mo and W derivatives, the reports in which mode of inhibition and K_i values have been defined are still very limited. A possible factor for this observation has been pointed out to be the much more complicated experimentation needed for determination of K_i which makes it a more demanding process than measuring EC_{50} or IC_{50} values [6].

In view of the above background, and our specific interest on biological activity of peroxoniobium compounds, we have decided to study the interaction of the

synthesized pNb complexes with phosphatase, using thylakoid membrane acid phosphatase as a model enzyme. One of the specific interests was to explore whether binding of low molecular weight pNb species to macromolecular ligands would alter their affinity as enzyme inhibitor.

Acid phosphatases, a group of membrane associated enzymes, catalyze the dephosphorylation of phosphate ester bond at an optimum pH of 4.9-6.0 and are widespread in nature [25]. Thylakoid membrane ACP is unique to photosynthesis, whereas human acid phosphatases, normally found at low concentrations, has been known to be diagnostically useful as serological and histological markers of diseases such as prostatic cancer and bone metastasis [26]. Apart from playing vital roles in diverse biological phenomena, these enzymes serve as excellent models to probe the metal induced inhibitory effect in membrane proteins [25,27,28].

Purple acid phosphatases (PAPs) in general consists of a dinuclear $Fe^{3+}M^{2+}$ center in their active site, with M = Fe^{2+} or Zn^{2+} or Mn^{2+} [29-34] of the type shown in **Fig.7.1** [35]. The two metal centers are coordinated by seven invariant ligands *i.e.*, one aspartate, one tyrosine and one histidine coordinated with Fe^{3+} and two histidines and one asparagine with M^{2+}, and an aspartate residue bridging the two ions (**Fig. 7.2**) [32].

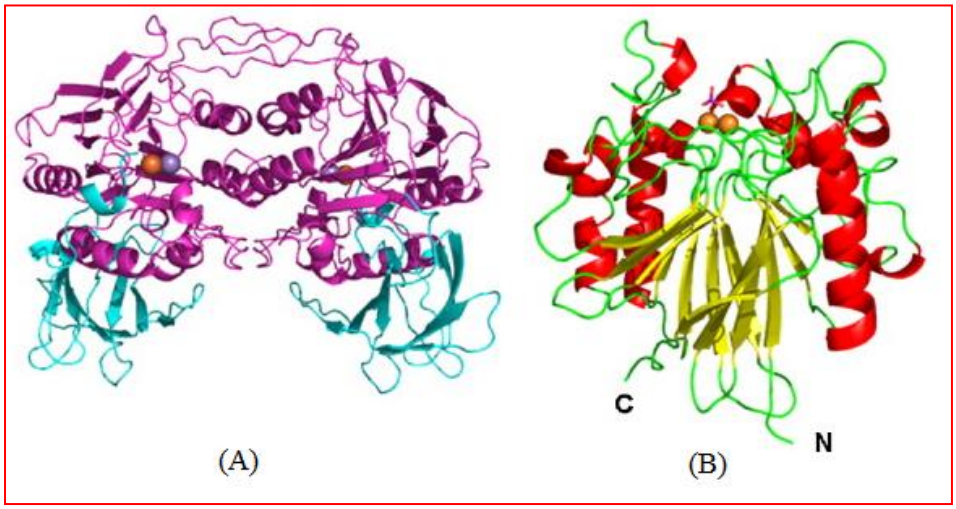

Fig. 7.1 General structures of plant (A) and animal (B) PAPs. Most of the plant PAPs reported to date are homodimeric with 55 kDa subunits whereas the animal PAPs studied to date are 35 kDa monomers. Each subunit has two domains *viz.*, an N-terminal domain without known function and a C-terminal domain that contains the active site [35].

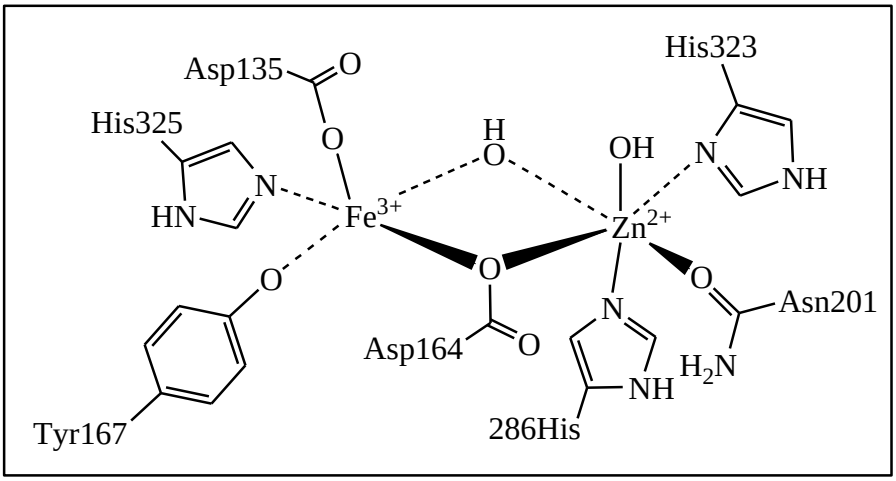

Fig. 7.2 Schematic of the active site of kidney bean purple acid phosphatase based on the 2.65-Å resolution structure described by Klabunde *et al.* [32].

The mammalian enzymes contain a dinuclear $Fe^{3+}Fe^{2+}$ center [36,37], while plant PAP from red kidney beans has an $Fe^{3+}Zn^{2+}$ center [38] *i.e.*, all PAPs have two metal ion binding sites in their catalytic center: (a) "chromophoric" site that binds trivalent ions, and (b) "redox active" site that binds divalent metal ions [35].

Presented in this chapter are the findings of our investigation on the steady state kinetic studies of the effect of the pNb complexes, *viz.*, monomeric homoleptic, **NaNb** and **KNb**, water soluble polymer anchored peroxoniobium compounds **3.1** and **3.2** as well as heteroleptic complexes **4.1-4.4**, on acid phosphatase *in vitro*.

7.2 Experimental section

7.2.1 Measurement of acid phosphatase activity

The acid phosphatase activity was assayed spectrophotometrically employing *p*-nitrophenyl phosphate (*p*-NPP) as a substrate [16,27,39,40]. In the standard assay, the reaction mixture contained acetate buffer (0.1 M, pH = 4.6), the enzyme (18.38 μg protein mL^{-1}) and different concentrations of monomeric pNb species, (concentration varies between 1 and 12 μM, as shown in **Fig. 7.3**) or the free ligand. For polymer bound compounds, the concentration varies between 2-10 μM for **PANb (3.1)** and 0.5-2 μM for **PSSNb (3.2)** as shown in **Fig. 7.3**. The reaction was started by addition of the substrate *p*-NPP to the test solution which was pre-incubated for 5 min. After 30 min of incubation

of the reaction solution at 30 °C, the reaction was terminated by addition of 0.9 mL of 0.5 M NaOH solution and the absorbance at 405 nm was recorded in order to determine the *p*-NP produced (molar extinction coefficient of the *p*-nitrophenolate =18000 $M^{-1}cm^{-1}$) [41]. The enzyme activity in the absence of the inhibitors was determined which was used as the control. The half-maximal inhibitory concentration of the inhibitor species giving 50% inhibition (IC_{50}) was determined graphically. All experiments were performed in triplicate. The data in the figures are presented as the mean ± SE from three separate experiments.

7.2.2 Determination of kinetic parameters

The kinetic constants, maximum velocity (V_{max}) and Michaelis constant (K_m) were determined from Lineweaver-Burk (L-B) plots following a rearrangement of the Michaelis-Menten equation [40,42,43] using Cary 100 Bio Enzyme Kinetics software.

$$\frac{1}{V} = \frac{K_m}{V_{max}[S]} + \frac{1}{V_{max}} \qquad \text{.....1}$$

In the present case, the following equation (2) was used to characterize the mode of inhibition, which was found to be of mixed type:

$$V = \left\{ \frac{V_{max} \times [S]}{K_m\left(\frac{1+[I]}{K_i}\right) + [S]\left(1 + \frac{[I]}{K_{ii}}\right)} \right\} \qquad \text{.....2}$$

where V is the velocity, $[S]$ is the *p*-NPP concentration and $[I]$ denotes the inhibitor concentration, K_i and K_{ii} are inhibitory constants for the competitive part and non competitive part, respectively. The enzyme inhibitor constants were determined from secondary plots of the initial rate data by a linear regression analysis. In order to obtain K_i, the slopes from the Lineweaver-Burk plots were re-plotted against the inhibitor concentration values from the x-intercepts of these re-plots. The K_{ii} was obtained from the plot of intercepts that has been found from the Lineweaver-Burk plots against the inhibitor concentration values from the x-intercepts of these re-plots.

7.3 Results and discussion

7.3.1 Inhibitory effect of pNb compounds on acid phosphatase

The *in vitro* phosphatase inhibitory effect of the triperoxoniobium compounds *viz.*, monomeric heteroleptic pNb compounds, **4.1-4.4** and macro complexes, **PANb (3.1)** and **PSSNb (3.2)** as well as parent tetraperoxoniobates, **NaNb** and **KNb** upon activity of the wheat thylakoid membrane ACP was evaluated employing standard enzyme assay system and *p*-NPP as substrate. A variety of enzyme assays have been made use of previously, to measure phosphatase inhibition by metal compounds such as vanadates, molybdates and tungstates [6,16,17,27,40]. The mode of enzyme inhibition such as competitive, non-competitive or mixed type can usually be ascertained [44] by varying the inhibitor concentration and measuring the enzyme activity at various substrate concentrations. The findings of our investigation on dose response inhibition of the model enzyme activity by the pNb complexes are illustrated in **Fig. 7.3.**

The inhibitor potential of the test compounds was quantified in terms of the half-maximal inhibitory concentration (IC_{50}). The IC_{50} values recorded, being within the range of 1-9 μM, implied that the compounds are highly potent inhibitors of the enzyme (**Fig. 7.3** and **Table 7.1**). While the IC_{50} value of tetraperoxo species was observed to be comparable to that displayed by triperoxoNb complexes with arginine (**NbA, 4.3)** and nicotinic acid (**NbN, 4.4)** as co-ligands, the compounds **NbAla (4.1)** and **NbVal** (**4.2)** were found to be relatively less potent. Significantly, the pNb compound supported on poly(styrene sulfonate) (**PSSNb, 3.2**) was observed to be the most efficient inhibitor of ACP among investigated pNb compounds with its IC_{50} value nearly 6 fold lower than the poly(acrylate) bound pNb complex. Thus the data obtained indicated the following sequence of inhibitor potency for ACP inhibition: **PSSNb >> NaNb > KNb > NbN > NbA > NbVal > PANb > NbAla**. Since individually the free ligands or polymers had no observable effect on the enzyme activity, under the employed assay conditions, the above observations indicate that the inhibitory effect of the pNb compounds indeed originate from the interaction of the intact metal complexes with the enzyme and the ligand environment influences the inhibitor potency of the tested complexes.

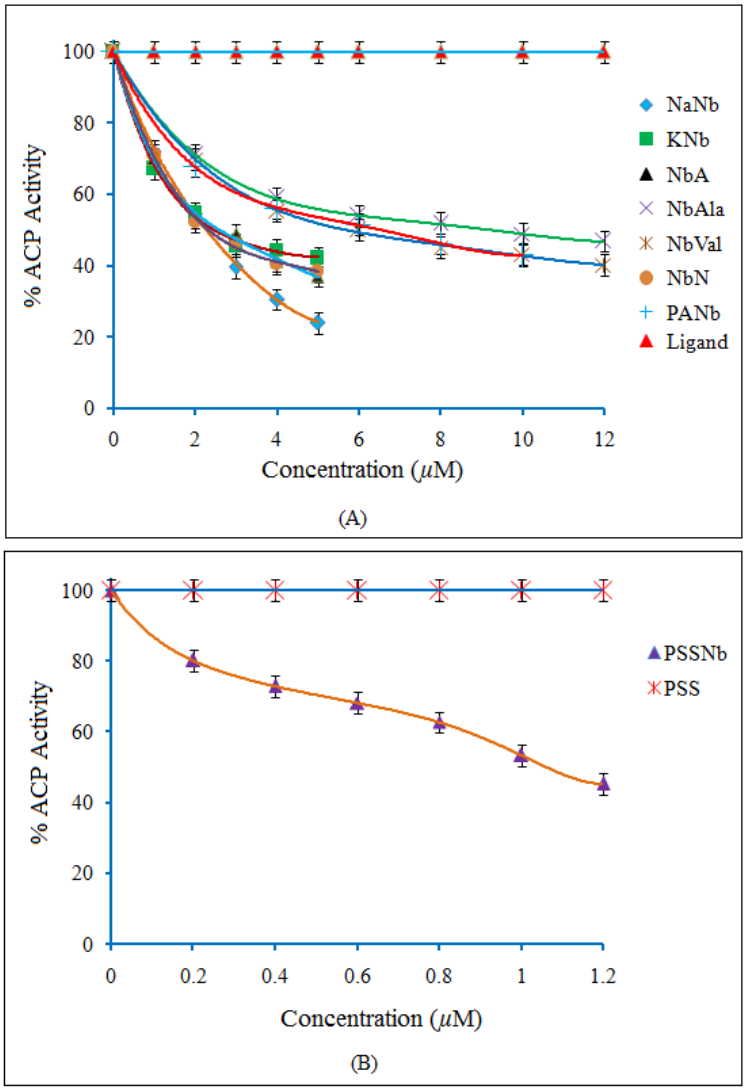

Fig. 7.3 The effect of synthesized pNb compounds and free ligand on the activity of ACP. The ACP catalyzed rates of hydrolysis of *p*-NPP at pH 4.6 were determined at 30 °C by measuring A_{405} in a reaction mixture containing ACP (18.38 μg mL^{-1}) and *p*-NPP (2 mM) in acetate buffer (0.1 M, pH = 4.6) in the absence or presence of stated concentrations of the inhibitors. (A) for **NaNb**, **NbA**, **NbN** and the respective free ligand, compound concentrations: 1, 2, 3, 4 and 5 μM and for **NbAla**, **NbVal** and the respective free ligand, compound concentration: 2, 4, 6, 8, 10 and 12 μM and for pNb macrocomplexes **PANb** and poly(sodium acrylate), compound concentration: 2, 4, 6, 8 and 10 μM and (B) for **PSSNb** and poly(sodium styrene sulfonate), compound concentration: 0.2, 0.4, 0.6, 0.8, 1.0 and 1.2 μM). The data are presented as the mean ±SE from three separate experiments. For polymeric compounds, the compound concentrations are on the basis of peroxometal loading.

7.3.2 Kinetics of ACP inhibition by the pNb complexes

To establish the mechanism of inhibition for the acid phosphatase catalyzed hydrolysis of *p*-NPP by the inhibitor species, the steady state kinetics of this process were investigated and kinetic parameters K_m and V_{max} were determined [40,42,43]. The L-B plots of the reciprocal initial velocity versus the reciprocal substrate concentration in the absence and presence of the inhibitor complexes at various concentrations are shown in **Fig. 7.4 (**for **NaNb**, **KNb**, **4.1** and **4.2)** and **Fig. 7.5** (for **4.3, 4.4, 3.1** and **3.2)**. Kinetic measurements yielded straight lines with point of intersection in the second quadrant in each case.

As can be readily seen in **Fig. 7.4** and **Fig. 7.5 (A, B)**, both V_{max} and K_m values are affected by the presence of each of the free pNb complexes showing an increase in K_m and decrease in velocity V_{max} values with increasing inhibitor concentration. This behaviour is characteristic of mixed type of inhibition combining competitive and non-competitive modes. On the other hand, an increase in concentration of each of the polymeric complexes resulted in decrease of V_{max} whereas K_m remained constant [**Fig. 7.5 (C, D)]** suggesting that the macro complexes are classical non-competitive inhibitors of ACP. The above observations are consistent with the mode of inhibition exhibited by monomeric and polymer anchored peroxo compounds of V, Mo and W reported previously from our laboratory [15-17].

We have also determined the inhibitor constants K_i and K_{ii} in order to assess the affinity of the enzyme for the inhibitors. The inhibitor constant K_i is a measure of the affinity of the inhibitor for the free enzyme whereas, K_{ii} reflects its affinity for the enzyme-substrate complex. The ratio of K_{ii} and K_i values were used to assess the relative competitiveness of each inhibitor. A larger K_{ii}/K_i value indicates a mixed type of inhibition that is relatively more competitive in its action, whereas a lower K_{ii}/K_i reflects the mixed type of inhibition that is more uncompetitive. On the other hand, when $K_{ii} = K_i$, the mode of inhibition becomes noncompetitive.

In the present study, as shown in the inset to **Fig. 7.4** and **Fig. 7.5 (A, B)**, the inhibitor constant K_i for the competitive part of inhibition, was obtained from the secondary plot of the slope of the primary plot ($1/V$ versus $1/[S]$) against the inhibitor concentration with the intercept on the inhibitor axis being $-K_i$. The value of K_{ii}, inhibitor

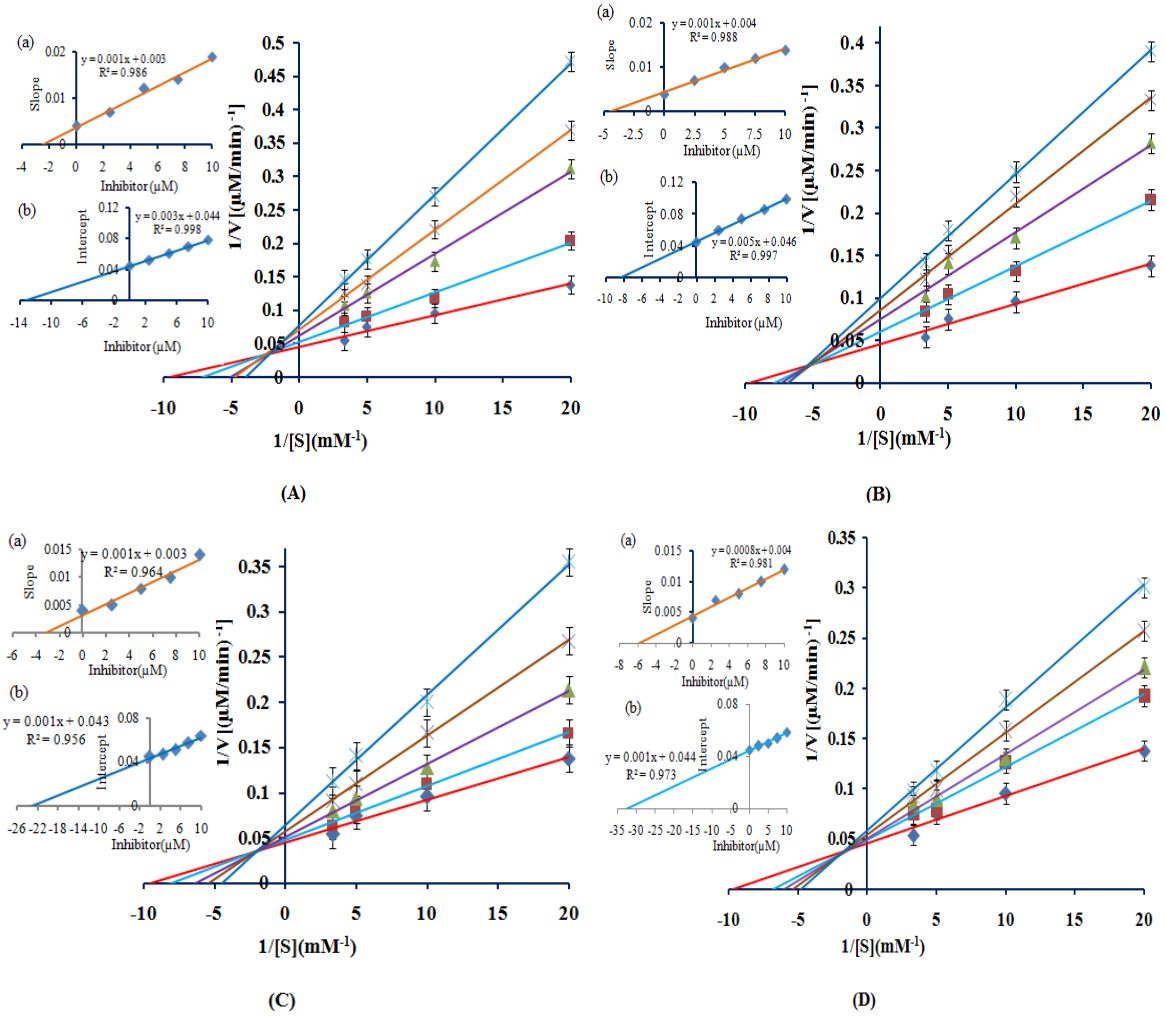

Fig. 7.4 Lineweaver-Burk plots for the inhibition of ACP activity in the absence and presence of (A) **NaNb**, (B) **KNb,** (C) **NbAla** and (D) **NbVal**. The inset represents the secondary plot of the initial kinetic data of the Lineweaver-Burk plot. The reaction mixture contained acetate buffer (0.1 M, pH 4.6) and *p*-NPP (50-300 μM). The reaction was started by adding ACP (18.38 μg mL^{-1}) to the reaction solution, which was pre-incubated for 5 min and the rates of hydrolysis in the presence of ♦ 0 μM, ■ 2.5μM, ▲ 5 μM, X 7.5 μM, ж 10 μM inhibitors were obtained. The values are expressed as the mean ± SE from three separate experiments. Inset: (a) the slopes were plotted against inhibitor concentrations and K_i values were obtained from the x-intercepts of these re-plots. (b) The vertical intercepts were plotted against the inhibitor concentration and K_{ii} values were obtained from the x-intercepts of these re-plots.

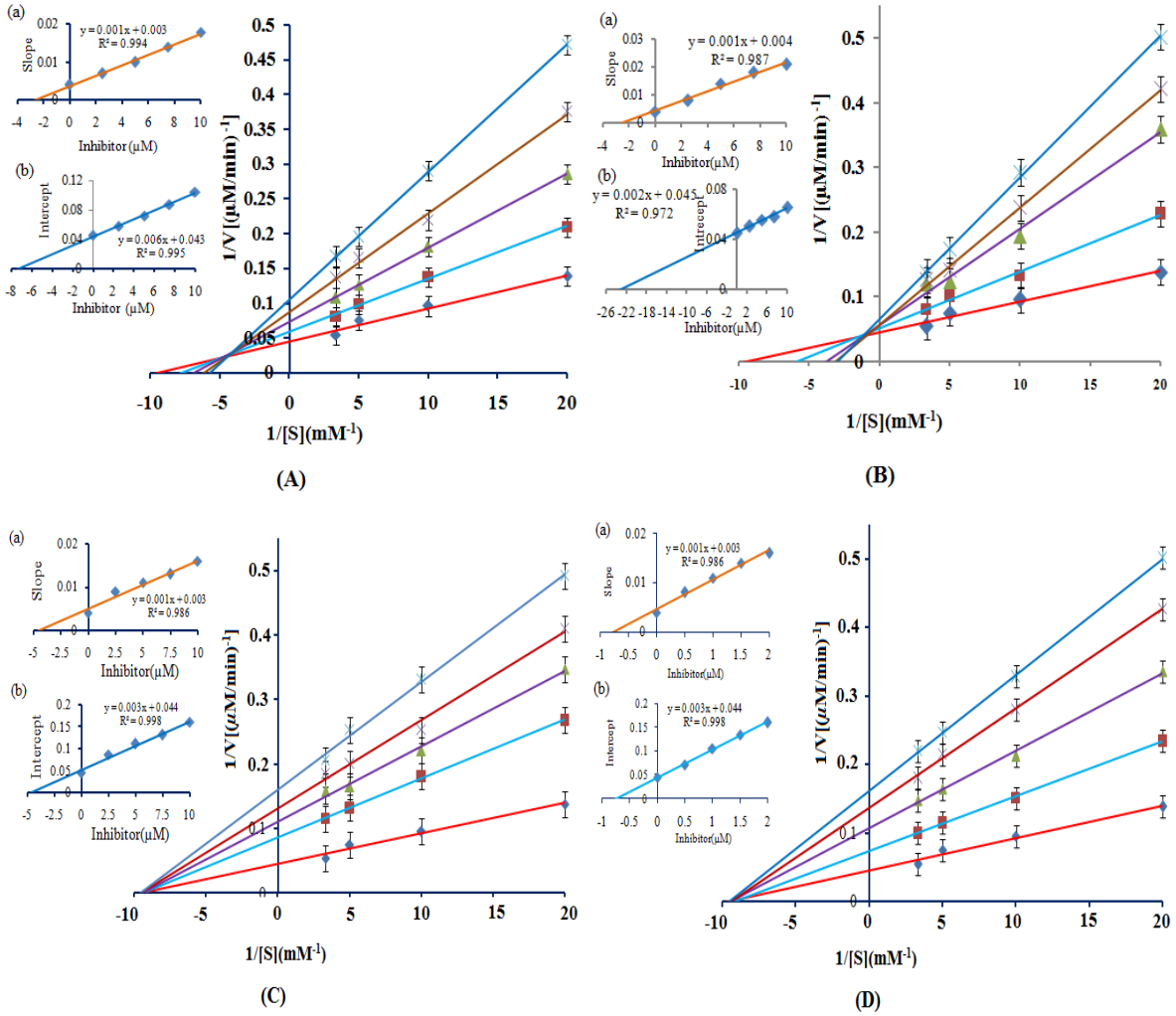

Fig. 7.5 Lineweaver-Burk plots for the inhibition of ACP activity in the absence and presence of (A) **NbA**, (B) **NbN** (C) **PANb** and (D) **PSSNb**. The inset represents the secondary plot of the initial kinetic data of the Lineweaver-Burk plot. The reaction mixture contained acetate buffer (0.1 M, pH 4.6) and *p*-NPP (50-300 μM). The reaction was started by adding ACP (18.38 μg mL^{-1}) to the reaction solution, which was pre-incubated for 5 min and the rates of hydrolysis in the presence of ♦ 0 μM, ■ 2.5μM, ▲ 5 μM, X 7.5 μM, ж 10 μM inhibitors were obtained. The values are expressed as the mean ± SE from three separate experiments. Inset: (a) the slopes were plotted against inhibitor concentrations and K_i values were obtained from the x-intercepts of these re-plots. (b) The vertical intercepts were plotted against the inhibitor concentration and K_{ii} values were obtained from the x-intercepts of these re-plots. For polymeric compound concentrations are on the basis of peroxometal loading.

constant for non-competitive inhibition, was obtained from the replot of slope versus inhibitor concentration, with the inhibitor axis intercept being equivalent to $-K_{ii}$. The kinetic results observed for monomeric pNb compounds (**Table 7.1**), show that for each of the inhibitors $K_{ii} > K_i$, confirming that pNb species exert mixed type of inhibition on ACP activity. On the contrary, for each of the macromolecular complexes, *viz.*, **PANb** and **PSSNb** [**Fig. 7.5 (C, D)**, and **Table 7.1**], the value of K_i was observed to be nearly equal to K_{ii}, which is characteristic of a non-competitive inhibitor.

A competitive inhibitor is known to share a close structural resemblance to the natural substrate of the enzyme whereas, a non-competitive inhibitor binds reversibly at a site far removed from the active site causing a conformational change in the overall three-dimensional shape of the enzyme [16]. The trend emerging out of our present study demonstrates that the compounds tested can be grouped into two categories on the basis

Table 7.1 Half-maximal inhibitory concentration (IC_{50}) and inhibitor constants (K_i and K_{ii}) values for pNb compounds

Compound	IC_{50} (μM)	K_i(μM)	K_{ii}(μM)	K_{ii}/K_i	Types of inhibition
NaNb	2.24	2.75	12.85	4.67	Mixed inhibition
KNb	2.30	4.2	8.5	2.02	Mixed inhibition
NbA	2.59	2.70	7.10	2.63	Mixed inhibition
NbN	2.35	2.45	22.90	9.35	Mixed inhibition
NbAla	8.85	3.15	22.20	7.05	Mixed inhibition
NbVal	5.65	5.60	32.45	5.79	Mixed inhibition
PANb	6.55	4.3	4.5	1.05	Non-competitive
PSSNb	1.06	0.72	0.73	1.01	Non-competitive

[a]Note: the ACP catalyzed rates of hydrolysis of *p*-NPP at pH 4.6 were determined at 30 °C by measuring A_{405} in a reaction mixture containing ACP (18.38 μg mL^{-1}) and *p*-NPP (50-300 μM) in acetate buffer (0.1 M, pH = 4.6) in the presence of stated concentrations of the inhibitors (as shown in **Fig. 7.4** and **Fig. 7.5**).

of mode of ACP inhibition. The first group comprising of free monomeric pNb compounds exerts mixed inhibition indicating the presence of both competitive and non-competitive binding sites, whereas, the polymer bound metal peroxo compounds are classical non-competitive inhibitors of the phosphoproteins. Previous reports on phosphatase inhibition by V and pV compounds, have suggested that in addition to the nature of the enzyme, one or more of the various factors such as oxidation state of the metal, co-ordination geometry and stability of the compounds under physiological condition may be responsible in deciding the phosphatase inhibitory ability of the compound [45,46].

Acid phosphatases, isolated from various plant and animal sources, as has been already mentioned, contain dinuclear iron active sites and highly conserved amino acid sequences with a histidine residue at the active site [26,27,47-50]. Oxy anions of V, Mo and W having penta or hexa co-ordinated structures have mostly been known to be competitive inhibitors of phosphatases due to their structural analogy with phosphate. However, with respect to inhibition of acid phosphatases, different oxometallates have been shown to display different mechanistic preferences ranging from competitive, non-competitive to uncompetitive patterns of inhibition [16,51-54]. The work of Vincent and co-workers [47] demonstrated that oxyanions such as molybdate and tungstate being relatively larger in size, bind in a non-competitive fashion by bridging the two iron atoms in the binuclear active site of mammalian ACP, while the smaller anions may also bind at a single iron atom in a competitive manner. Oxidative interaction between the highly oxidative compounds with the Fe^{2+} centre resulting in its oxidation to ferric form and consequent inactivation of the enzyme in a non-competitive manner was suggested as an additional possibility of inhibitory effect of these complexes [47]. It is already evident from the results presented in Chapter 5, the pNb compounds under investigation are efficient oxidants of organic substrates. In view of these observations it is reasonable to expect that in the present study too, a similar mechanism involving oxidation of Fe^{2+} centre by the pNb species is perhaps operative, contributing to their mixed type of inhibition of ACP function, combining competitive and non-competitive pathways. Macromolecular complexes on the other hand, due to their larger size, are likely to interact with the enzyme at a site away from the active site which may result in change in

overall conformation of the protein and inhibition of its function in a non-competitive manner [47].

However, in the absence of direct evidence and due to the complicated chemistry and intricacy of the interactions between pNb species and complex biomolecules involved in the present study, it is difficult to comment on the exact mechanism of inhibition at this stage. Nevertheless, there are ample evidences in the literature highlighting the importance of redox properties of pV compounds in inhibition of protein phosphatases [14,45] which lend credence to our hypothesis.

7.4 Conclusion

To summarize, our experiments confirm that the pNb complexes tested, irrespective of their ligand environment, induce a strong inhibitory effect on acid phosphatase activity. Detailed inhibition kinetics studies demonstrated that each of the monomeric pNb compounds is a potent mixed-type of inhibitor of the enzyme, combining competitive and non-competitive modes of inhibition. In contrast, pNb macro-complexes served as classic non-competitive inhibitors of ACP. That the macro complexes and the monomeric pNb compounds inhibit the enzyme function *via* distinct pathways is thus clearly evident. It is notable that with respect to mechanism of inhibition, similar observations have been made previously in case of acid as well as alkaline phosphatase inhibition by peroxo compounds of V(V), Mo(VI) and W(VI) [15-17]. On the basis of the collective findings from our present study along with the results of our previous investigations, it may be expected that the immobilized peroxometallates may serve as promising systems as selective probes of non-competitive site of inhibition of phosphatases.

References

1. In Seibel, M. J., Robins, S. P., and Bilezikian, J. P., editors, *Dynamics of Bone and Cartilage Metabolism: Principles and Clinical Applications*. Academic Press, 2006.
2. Hunter, T. Why nature chose phosphate to modify proteins. *Philosophical Transactions of the Royal society B*, 367(1602):2513-2516, 2012.
3. Torres, E. and Rosen, M. K. Contingent phosphorylation/dephosphorylation provides a mechanism of molecular memory in WASP. *Molecular Cell*, 11(5):1215-1227, 2003.
4. Tanaka, N., Hasan, Z., Hartog, A. F., van Herk, T., and Wever, R. Phosphorylation and dephosphorylation of polyhydroxycompounds by class A bacterial acid phosphatases. *Organic & Biomolecular Chemistry*, 1(16):2833-2839, 2003.
5. Saltiel, A. R. New perspectives into the molecular pathogenesis and treatment of type 2 diabetes. *Cell*, 104(4):517-529, 2001.
6. McLauchlan, C. C., Peters, B. J., Willsky, G. R., and Crans, D. C. Vanadium-phosphatase complexes: Phosphatase inhibitors favor the trigonalbipyramidal transition state geometries. *Coordination Chemistry Reviews*, 301:163-199, 2015.
7. Hunter, T. Protein kinases and phosphatases: the yin and yang of protein phosphorylation and signaling. *Cell*, 80(2):225-236, 1995.
8. Hunter, T. Signaling-2000 and beyond. *Cell*, 100(1):113-127, 2000.
9. McConnell, J. L. and Wadzinski, B. E. Targeting protein serine/threonine phosphatases for drug development. *Molecular Pharmacology*, 75(6):1249-1261, 2009.
10. Shaver, A., Ng, J. B., Hall, D. A., and Posner, B. I. The chemistry of peroxovanadium compounds relevant to insulin mimesis. *Molecular and Cellular Biochemistry*, 153(1):5-15, 1995.
11. Shechter, Y., Goldwaser, I., Mironchik, M., Fridkin, M., and Gefel, D. Historic perspective and recent developments on the insulin-like actions of vanadium; toward developing vanadium-based drugs for diabetes. *Coordination Chemistry Reviews*, 237(1):3-11, 2003.
12. Cantley, L. C., Josephson, L., Warner, R., Yanagisawa, M., Lechene, C., and Guidotti, G. Vanadate is a potent (Na, K)-ATPase inhibitor found in ATP derived from muscle. *Journal of Biological Chemistry*, 252(21):7421-7423, 1977.

13. Kustin, K. Perspective on vanadium biochemistry. In Tracy, A. S. and CransD.C., editors, *Vanadium Compounds Chemistry, Biochemistry, and Therapeutic Applications*, pages 170-185. Oxford University Press, UK, 1998.
14. Crans, D. C., Smee, J. J., Gaidamauskas, E., and Yang, L. The chemistry and biochemistry of vanadium and the biological activities exerted by vanadium compounds. *Chemical Reviews*, 104(2):849-902, 2004.
15. Islam, N. S. and Boruah, J. J. Macromolecular peroxo complexes of vanadium(V) and molybdenum(VI): Catalytic activities and biochemical relevance. *Journal of Chemical Sciences*, 127(5):777-795, 2015.
16. Das, S. P., Ankireddy, S. R., Boruah, J. J., and Islam, N. S. Synthesis and characterization of peroxotungsten(VI) complexes bound to water soluble macromolecules and their interaction with acid and alkaline phosphatases. *RSC Advances*, 2(18):7248-7261, 2012.
17. Boruah, J. J., Kalita, D., Das, S. P., Paul, S., and Islam, N. S. Polymer-anchored peroxo compounds of vanadium(V) and molybdenum(VI): synthesis, stability, and their activities with alkaline phosphatase and catalase. *Inorganic Chemistry*, 50(17):8046-8062, 2011.
18. Kalita, D., Das, S. P., and Islam, N. S. Kinetics of inhibition of rabbit intestine alkaline phosphatase by heteroligand peroxo complexes of vanadium(V) and tungsten(VI). *Biological Trace Element Research*, 128(3):200-219, 2009.
19. Hazarika, P., Kalita, D., and Islam, N. S. Mononuclear and dinuclear peroxotungsten complexes with co-ordinated dipeptides as potent inhibitors of alkaline phosphatase activity. *Journal of Enzyme Inhibition and Medicinal Chemistry*, 23(4):504-513, 2008.
20. Hazarika, P., Kalita, D., Sarmah, S., and Islam, N. S. New oxo-bridged peroxotungsten complexes containing biogenic co-ligand as potent inhibitors of alkaline phosphatase activity. *Molecular and Cellular Biochemistry*, 284(1):39-47, 2006.
21. Fraqueza, G., Ohlin, C. A., Casey, W. H., and Aureliano, M. Sarcoplasmic reticulum calcium ATPase interactions with decaniobate, decavanadate, vanadate, tungstate and molybdate. *Journal of Inorganic Biochemistry*, 107(1):82-89, 2012.

22. In Srivastava, A. K. and Chiasson, J. L., editors, *Vanadium Compounds: Biochemical and Therapeutic Applications*, volume 16. Springer Science & Business Media, 2012.
23. Thompson, K. H., Lichter, J., LeBel, C., Scaife, M. C., McNeill, J. H., and Orvig, C. Vanadium treatment of type 2 diabetes: A view to the future. *Journal of Inorganic Biochemistry*, 103(4):554-558, 2009.
24. Pessoa, J. C., Etcheverry, S., and Gambino, D. Vanadium compounds in medicine. *Coordination Chemistry Reviews*, 301:24-48, 2015.
25. Wilcox, D. E. Binuclear metallohydrolases. *Chemical Reviews*, 96(7):2435-2458, 1996.
26. Bull, H., Murray, P. G., Thomas, D., Fraser, A. M., and Nelson, P. N. Acid phosphatases. *Journal of Clinical Pathology*, 55(2):65, 2002.
27. Fei, M. J., Chen, J. S., and Wang, X. Y. Biochemical properties and inhibition kinetics of phosphatase from wheat thylakoid membranes. *Journal of Integrative Plant Biology*, 48(3):294-299, 2006.
28. Lipscomb, W. N. and Sträter, N. Recent advances in zinc enzymology. *Chemical Reviews*, 96(7):2375-2434, 1996.
29. Araujo, C. L. and Vihko, P. T. Structure of acid phosphatases. *Phosphatase Modulators*, 155-166, 2013.
30. Que, L. and True, A. E. Dinuclear iron-and manganese-oxo sites in biology. *Progress in Inorganic Chemistry: Bioinorganic Chemistry*, 38:97-200, 1990.
31. Vincent, J. B., Olivier-Lilley, G. L., and Averill, B. A. Proteins containing oxo-bridged dinuclear iron centers: a bioinorganic perspective. *Chemical Reviews*, 90(8):1447-1467, 1990.
32. Klabunde, T., Strater, N., Fralich, R., witzel, H., and Krebs, B. Mechanism of Fe(III)-Zn(II) purple acid phosphatase based on crystal structure. *Journal of Molecular Biology*, 259:737-748, 1996.
33. Schenk, G., Ge, Y., Carrington, L. E., Wynne, C. J., Searle, I. R., Carroll, B. J., Hamilton, S., and de Jersey, J. Binuclear metal centers in plant purple acid phosphatases: Fe-Mn in sweet potato and Fe-Zn in soybean. *Archives of Biochemistry and Biophysics*, 370(2):183-189, 1999.
34. Schenk, G., Boutchard, C. L., Carrington, L. E., Noble, C. J., Moubaraki, B., Murray, K. S., de Jersey, J., Hanson, G. R., and Hamilton, S. A purple acid phosphatase from

sweet potato contains an antiferromagnetically coupled binuclear Fe-Mncenter. *Journal of Biological Chemistry*, 276(22):19084-19088, 2001.

35. Schenk, G., Mitić, N., Hanson, G. R., and Comba, P. Purple acid phosphatase: A journey into the function and mechanism of a colorful enzyme. *Coordination Chemistry Reviews*, 257(2):473-482, 2013.
36. Antanaitis, B. C., Aisen, P., and Lilienthal, H. R. Physical characterization of two-iron uteroferrin. Evidence for a spin-coupled binuclear iron cluster. *Journal of Biological Chemistry*, 258(5):3166-3172, 1983.
37. Averill, B. A., Davis, J. C., Burman, S., Zirino, T., Sanders-Loehr, J., Loehr, T. M., Sage, J. T., and Debrunner, P. G. Spectroscopic and magnetic studies of the purple acid phosphatase from bovine spleen. *Journal of the American Chemical Society*, 109(12):3760-3767, 1987.
38. Beck, J. L., McConachie, L. A., Summors, A. C., Arnold, W. N., De Jersey, J., and Zerner, B. Properties of a purple phosphatase from red kidney bean: a zinc-iron metalloenzyme. *Biochimica et Biophysica Acta (BBA)-Protein Structure and Molecular Enzymology*, 869(1):61-68, 1986.
39. Albrecht, R., Le Petit, J., Calvert, V., Terrom, G., and Périssol, C. Changes in the level of alkaline and acid phosphatase activities during green wastes and sewage sludge co-composting. *Bioresource Technology*, 101(1):228-233, 2010.
40. Bergmeyer, H. U., Bergmeyer, J., and Grassl, M. *Methods of Enzymatic Analysis*, third ed. Verlag Chemie, Weinheim, Deerfield Beach, FL, 1983.
41. Ferreira, C. V., Taga, E. M., and Aoyama, H. Glycolytic intermediates as substrates of soybean acid phosphatase isoforms. *Plant Science*, 147(1):49-54, 1999.
42. Lineweaver, H. And Burk, D. The determination of enzyme dissociation constants. *Journal of the American Chemical Society*, 56(3):658-666, 1934.
43. Cornish-Bowden, A. Current IUBMB recommendations on enzyme nomenclature and kinetics. *Perspectives in Science*, 1(1):74-87, 2014.
44. Segel, I. H. *Enzyme Kinetics: Behavior and Analysis of Rapid Equilibrium and Steady State Enzyme Systems.* Wiley, New York, 1975.
45. Crans, D. C. In Tracey, A. S. and Crans, D. C., editors, *Vanadium Compounds: Chemistry, Biochemistry, and Therapeutic Applications*, pages 82-103. Oxford University Press, UK, 1998.

46. Louie, A. Y. and Meade, T. J. Metal complexes as enzyme inhibitors. *Chemical Reviews*, 99(9):2711-2734, 1999.
47. Vincent, J. B., Crowder, M. W., and Averill, B. A. Spectroscopic and kinetics studies of a high-salt-stabilized form of the purple acid phosphatase from bovine spleen. *Biochemistry*, 30(12):3025-3034, 1991.
48. Hunt, D. F., Yates, J. R., Shabanowitz, J., Zhu, N. Z., Zirino, T., Averill, B. A., Daurat-Larroque, S. T., Shewale, J. G., Roberts, R. M., and Brew, K. Sequence homology in the metalloproteins; purple acid phosphatase from beef spleen and uteroferrin from porcine uterus. *Biochemical and Biophysical Research Communications*, 144(3):1154-1160, 1987.
49. Ketcham, C. M., Roberts, R. M., Simmen, R. C., and Nick, H. S. Molecular cloning of the type 5, iron-containing, tartrate-resistant acid phosphatase from human placenta. *Journal of Biological Chemistry*, 264(1):557-563, 1989.
50. Lord, D. K., Cross, N. C., Bevilacqua, M. A., Rider, S. H., Gorman, P. A., Groves, A. V., Moss, D. W., Sheer, D., and Cox, T. M. Type 5 acid phosphatase. *The FEBS Journal*, 189(2):287-293, 1990.
51. Stankiewicz, P. J. and Gresser, M. J. Inhibition of phosphatase and sulfatase by transition-state analogues. *Biochemistry*, 27(1): 206-212, 1988.
52. Heo, Y. S., Ryu, J. M., Park, S. M., Park, J. H., Lee, H. C., Hwang, K. Y., and Kim, J. S. Structural basis for inhibition of protein tyrosine phosphatases by Keggin compounds phosphomolybdate and phosphotungstate. *Experimental and Molecular Medicine*, 34(3):211-223, 2002.
53. VanEtten, R. L., Waymack, P. P., and Rehkop, D. M. Transition metal ion inhibition of enzyme-catalyzed phosphate ester displacement reactions. *Journal of the American Chemical Society*, 96(21):6782-6785, 1974.
54. Soman, G., Chang, Y. C., and Graves, D. J. Effect of oxyanions of the early transition metals on rabbit skeletal muscle phosphorylase. *Biochemistry*, 22(21):4994-5000, 1983.